

Computations of three-body continuum spectra

A. Cobis, D. V. Fedorov and A. S. Jensen
Institute of Physics and Astronomy,
Aarhus University, DK-8000 Aarhus C, Denmark

Abstract

We formulate a method to solve the coordinate space Faddeev equations for positive energies. The method employs hyperspherical coordinates and analytical expressions for the effective potentials at large distances. Realistic computations of the parameters of the resonances and the strength functions are carried out for the Borromean halo nucleus ${}^6\text{He}$ ($n+n+\alpha$) for $J^\pi = 0^\pm, 1^\pm, 2^\pm$.

PACS numbers: 21.45.+v, 11.80.Jy, 31.15.Ja, 21.60.Gx

Introduction. The three-body continuum problem has been the subject of numerous investigations [1]. Tremendous progress has been achieved, but still a number of problems remain [2]. Many approximate solutions have been invented without an emerging established general procedure. Different treatments are usually needed for short-range and long-range interactions and for energies below or above possible two-body thresholds [3, 4, 5]. It is necessary, but not always easy, to distinguish between inaccurate numerical results and shortcomings of the basic interactions.

During the last decade a new class of weakly bound three-body systems, nuclear halos, attracted enormous attention [6, 7, 8]. If no binary subsystem is bound, they are called Borromean nuclei. These concepts are general and of interest in many subfields of physics [9, 10]. Accumulating data from such systems demand analyses heavily relying on the properties of their continuum spectra [11, 12]. However, technical difficulties related to the precise behavior at large distance are substantial and so far unsolved.

Recently a new method with explicit analytical treatment of the large distances [13, 14] was used to obtain bound-state solutions to the Faddeev equations. The method is very powerful as seen by the successful investigation of the Efimov effect [9, 15]. The purpose of this letter is to generalize the method to obtain continuum state solutions. In order to illustrate the efficiency of the method we perform a realistic computation of a three-body Borromean halo system.

Method. The k 'th particle has mass m_k and coordinate \mathbf{r}_k . The two-body potentials are V_{ij} . We shall use the three sets of Jacobi coordinates $(\mathbf{x}_i, \mathbf{y}_i)$ and the corresponding three sets of hyperspherical coordinates $(\rho, \alpha_i, \Omega_{xi}, \Omega_{yi})$ [7, 8, 15]. The kinetic energy operator is then

$$T = \frac{\hbar^2}{2m} \left(-\rho^{-5/2} \frac{\partial^2}{\partial \rho^2} \rho^{5/2} + \frac{15}{4\rho^2} + \frac{\hat{\Lambda}^2}{\rho^2} \right), \quad (1)$$

$$\hat{\Lambda}^2 = -\frac{1}{\sin(2\alpha)} \frac{\partial^2}{\partial \alpha^2} \sin(2\alpha) + \frac{\hat{l}_x^2}{\sin^2 \alpha} + \frac{\hat{l}_y^2}{\cos^2 \alpha} - 4, \quad (2)$$

where the angular momentum operators \hat{l}_x^2 and \hat{l}_y^2 are related to the \mathbf{x} and \mathbf{y} degrees of freedom.

The total wave function is now expanded in a complete set of hyperangular functions

$$\Psi(\rho, \Omega) = \frac{1}{\rho^{5/2}} \sum_{n=1}^{\infty} f_n(\rho) \sum_{i=1}^3 \frac{\phi_n^{(i)}(\rho, \Omega_i)}{\sin(2\alpha_i)}, \quad (3)$$

Each of the three components $\phi_n^{(i)}$ is expressed in the corresponding system of Jacobi coordinates and they satisfy for each ρ the three Faddeev equations

$$(\hat{\Lambda}^2 - \lambda_n) \frac{\phi_n^{(i)}}{\sin(2\alpha_i)} + \frac{2m}{\hbar^2} \rho^2 V_{jk} \sum_{l=1}^3 \frac{\phi_n^{(l)}}{\sin(2\alpha_l)} = 0, \quad (4)$$

where $\{i, j, k\}$ is a permutation of $\{1, 2, 3\}$. In the absence of bound subsystems the eigenvalues λ_n approach at large distances the hyperspherical spectrum obtained for $V_{jk} = 0$, i.e. $\lambda_n(\rho \rightarrow \infty) = K_n(K_n + 4)$, where K_n is odd or even natural numbers depending on the parity.

The expansion coefficients $f_n(\rho)$ satisfy the equations

$$\begin{aligned} & \left(-\frac{\partial^2}{\partial \rho^2} + \frac{\lambda_n + 15/4}{\rho^2} - Q_{nn} - \frac{2mE}{\hbar^2} \right) f_n(\rho) \\ & = \sum_{n' \neq n} \left(Q_{nn'} + 2P_{nn'} \frac{\partial}{\partial \rho} \right) f_{n'}(\rho). \end{aligned} \quad (5)$$

The coupling terms P and Q approach zero at least as fast as ρ^{-3} . For Borromean systems we can then choose those solutions $\Psi_{n'}$ to eq.(3) where the large-distance ($\rho \rightarrow \infty$) boundary conditions for $f_n^{(n')}$ are given by [16]

$$f_n^{(n')}(\rho) \rightarrow \delta_{n,n'} F_n^{(-)}(\kappa\rho) - S_{n,n'} F_n^{(+)}(\kappa\rho), \quad (6)$$

where $\kappa^2 = 2mE/\hbar^2$ and $F_n^{(\pm)}$ are related to the Hankel functions of integer order by

$$\begin{aligned} F_n^{(\pm)}(\kappa\rho) &= \sqrt{\frac{m\rho}{4\hbar^2}} H_{K_n+2}^{(\pm)}(\kappa\rho) \\ &\rightarrow \sqrt{\frac{m}{2\pi\kappa\hbar^2}} \exp\left[\pm i\kappa\rho \pm \frac{i\pi}{2}\left(K_n + \frac{3}{2}\right)\right]. \end{aligned} \quad (7)$$

The continuum wave functions are orthogonal and normalized to delta functions in energy.

By diagonalization of the S -matrix we obtain eigenfunctions and eigenphases. The phase shifts reveal the continuum structure of the system. In particular, a rapid variation with energy indicates a resonance. A precise computation of resonances and related widths can be done by use of the complex energy method, where eq.(5) is solved for $E = E_r - i\Gamma/2$ with the boundary condition $f_n^{(n')} = \delta_{n,n'} \sqrt{\frac{m\rho}{4\hbar^2}} H_{K_n+2}^{(+)}(\kappa\rho)$. These solutions correspond to poles of the S -matrix [16].

Large-distance behavior. Eq.(4) can be solved for large distances, where for short-range potentials all partial waves, except s-waves, decouple. We expand each component on the hyperspherical basis with the quantum numbers $\{l_x, l_y, L, s_x, s_y, S, J\}$ where L,S and J are the total orbital angular momentum, total spin and total angular momentum, respectively. We express two of the Faddeev components (j, k) in the coordinates related to the third Jacobi set (i) and project out the partial wave with a given set of angular momentum quantum numbers. This operation, leading from the i 'th to the j 'th Jacobi coordinates, is denoted by $R_{i,j}$.

For large ρ only small α contribute to the terms proportional to $V_{jk}(r_i)$ in eq.(4). This is due to the assumption of short-range potentials and because $r_i \propto \rho \sin \alpha_i$. Let us first explicitly consider the three coupled components, $\phi_L^{(i)}$, characterized by $l_{xi} = 0$ and $l_{yi} = L$ and therefore with the same total orbital angular momentum L and furthermore with the same spin structure. We expand in powers of α_i and find the leading order contribution from the transformation of such terms to be

$$R_{i,j} \left[\frac{\phi_L^{(j)}(\rho, \alpha_j)}{\sin(2\alpha_j)} \right] \simeq \frac{(-1)^L \phi_L^{(j)}(\rho, \varphi_{j,i})}{\sin(2\varphi_{j,i})}, \quad (8)$$

$$\tan \varphi_{i,j} = (-1)^p \sqrt{\frac{m_k(m_i + m_j + m_k)}{m_i m_j}}, \quad (9)$$

where p is the parity of the permutation $\{i, j, k\}$. Non-zero l_{xi} -values had produced higher powers of α_i in eq.(8). Thus, the eigenvalues λ related to the other

partial waves decouple at large distances and approach the hyperspherical spectrum. These waves assume the asymptotic behavior on a distance scale defined by the range of the interactions. On the other hand the s-waves couple and feel consequently the interactions over a distance defined by the scattering lengths.

We shall now concentrate on a system consisting of two neutrons and a spin-zero core. This model directly applies to ${}^6\text{He}$, a halo nucleus for which a large amount of experimental data exists. The model is also a good approximation for another halo nucleus, ${}^{11}\text{Li}$ [8].

Due to the antisymmetry between neutrons the three coupled components ($l_{xi} = 0, l_{yi} = L, i = 1, 2, 3$) reduce to two and the angular Faddeev equations eq.(4) are to leading order in α (large ρ) given by

$$\begin{aligned} & \left(-\frac{\partial^2}{\partial \alpha_1^2} + \frac{L(L+1)}{\cos^2 \alpha_1} + \rho^2 v_{\text{NN}}(\rho \sin \alpha_1) - \nu^2 \right) \\ & \times \phi_L^{(1)}(\rho, \alpha_1) = -2\alpha_1(-1)^L \rho^2 v_{\text{NN}}(\rho \sin \alpha_1) C_L^{(1)}, \\ & \left(-\frac{\partial^2}{\partial \alpha_2^2} + \frac{L(L+1)}{\cos^2 \alpha_2} + \rho^2 v_{\text{Nc}}(\rho \sin \alpha_2) - \nu^2 \right) \\ & \times \phi_L^{(2)}(\rho, \alpha_2) = -2\alpha_2(-1)^L \rho^2 v_{\text{Nc}}(\rho \sin \alpha_2) C_L^{(2)}, \end{aligned} \quad (10)$$

where $\nu^2 = \lambda + 4$, $v_{\text{NN}}(x_1) = V_{23}(x_1/\mu_{23})2m/\hbar^2$, $v_{\text{Nc}}(x_2) = V_{13}(x_2/\mu_{13})2m/\hbar^2$, $m\mu_{jk}^2 = m_j m_k / (m_j + m_k)$,

$$C_L^{(1)} = 2 \frac{\phi_L^{(2)}(\rho, \varphi)}{\sin(2\varphi)}, C_L^{(2)} = \frac{\phi_L^{(1)}(\rho, \varphi)}{\sin(2\varphi)} + \frac{\phi_L^{(2)}(\rho, \tilde{\varphi})}{\sin(2\tilde{\varphi})}. \quad (12)$$

with $\varphi = \varphi_{12}$, $\tilde{\varphi} = \varphi_{23}$.

For large ρ the short range potentials $\rho^2 v(\rho \sin \alpha_i)$ vanish for all α_i except in a narrow region around zero. Due to this rescaling the effective range approximation becomes better with ρ increasing and therefore any potential with the same scattering length and effective range would lead to the same results. Let us then in the region of large ρ use square well potentials $V_{jk}(r) = -V_0^{(i)} \Theta(r < R_i)$, or equivalently expressed by the reduced quantities $v_{jk}(x) = -v_0^{(i)} \Theta(x < X_i = R_i \mu_{jk})$, where the parameters are adjusted to reproduce the given two-body scattering lengths and effective ranges. The corresponding solutions are then accurate approximations to our original problem at distances larger than $2R_i$ [17].

The potentials $v(\rho \sin \alpha_i)$ are zero when $\alpha_i > \alpha_0^{(i)} \equiv \arcsin(X_i/\rho)$. Then eqs.(10-11) are especially simple, i.e.

$$\left(-\frac{\partial^2}{\partial \alpha_i^2} + \frac{L(L+1)}{\cos^2 \alpha_i} - \nu^2 \right) \phi_L^{(i)}(\rho, \alpha_i) = 0 \quad (13)$$

and the solutions, vanishing at $\alpha_i = \pi/2$, are given by

$$\phi_L^{(i,II)}(\rho, \alpha_i) = A_L^{(i)} P_L(\nu, \alpha_i), \quad (14)$$

$$P_L(\nu, \alpha) \equiv \cos^L \alpha \left(\frac{\partial}{\partial \alpha} \frac{1}{\cos \alpha} \right)^L \sin \left[\nu \left(\alpha - \frac{\pi}{2} \right) \right]. \quad (15)$$

The potentials $v(\rho \sin \alpha_i)$ are for large ρ only finite when $\alpha_i < \alpha_0^{(i)} \ll 1$. Then eqs.(10) and (11) are

$$\begin{aligned} \left(-\frac{\partial^2}{\partial \alpha_i^2} + L(L+1) - \rho^2 v_0^{(i)} - \nu^2 \right) \phi_L^{(i)}(\rho, \alpha_i) = \\ + 2\alpha_i (-1)^L \rho^2 v_0^{(i)} C_L^{(i)}, \end{aligned} \quad (16)$$

where the wave functions in $C_L^{(i)}$ in eq.(12) must be $\phi_L^{(i,II)}$. The solutions to eq.(16) are then

$$\phi_L^{(i,I)}(\rho, \alpha) = B_L^{(i)} \sin(\kappa_i \alpha) - 2\alpha (-1)^L \frac{\rho^2 v_0^{(i)}}{\kappa_i^2} C_L^{(i)}, \quad (17)$$

$$\kappa_i^2 \equiv -[L(L+1) - \rho^2 v_0^{(i)} - \nu^2]. \quad (18)$$

Matching the solutions, eqs.(14) and (17), and their derivatives at $\alpha_i = \alpha_0^{(i)}$ gives a linear set of equations for $A_L^{(i)}$ and $B_L^{(i)}$. Physical solutions are then only obtained when the corresponding determinant is zero. This is the quantization condition for λ and the eigenvalue equation determining the asymptotic behavior of $\lambda(\rho)$.

Realistic computations for ${}^6\text{He}$. The practical implementation of the method is tested on ${}^6\text{He}$ considered as two neutrons and a ${}^4\text{He}$ -core. The two-body interactions reproduce accurately the s-, p- and d-phase shifts up to 20 MeV. Furthermore, a diagonal three-body force, $S_3 \exp(-\rho^2/b_3^2)$, is added in eq.(5) for fine tuning. The range of the three-body force is by its definition given in terms of the hyperradius. For ${}^6\text{He}$, $\rho=2$ fm and 3 fm correspond roughly to configurations where the neutrons respectively are at the surface of the α -particle and outside the surface by an amount equal to their own radius. The idea of using the three-body force is to include effects beyond those accounted for by the two-body interactions.

Several phase equivalent parametrizations are possible for each radial shape of the two-body potential. They differ in the number of two-body bound states of which the lowest s-state is occupied by the core neutrons and therefore subsequently has to be excluded in the computation. The results are very close after fine tuning by use of the three-body interaction [18]. We shall therefore only use the potentials without bound states. All possible s-, p- and d-waves are included

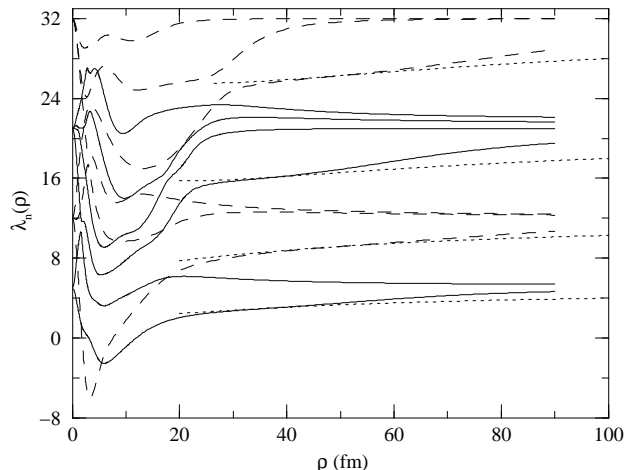


Figure 1: The lowest angular eigenvalues λ_n as function of ρ for angular momentum $J^\pi = 1^-$ (solid lines), and 2^+ (dashed lines) for ${}^6\text{He}$. The dotted lines are the large-distance asymptotic behavior. The neutron-neutron and the neutron- ${}^4\text{He}$ interactions are from [18] with $(V_c^{(l)}, r_c^{(l)}) = (48.2 \text{ MeV}, 2.33 \text{ fm}), (-47.40 \text{ MeV}, 2.30 \text{ fm}), (-21.93 \text{ MeV}, 2.03 \text{ fm})$ for s, p and d waves respectively. The spin orbit parameters are $(V_{so}, r_{so}) = (-25.49 \text{ MeV}, 1.72 \text{ fm})$. Maximum K_n -values up to 142 are used.

whereas other waves can be ignored to the accuracy we need. The number of Jacobi polynomials in the basis expansion is carefully chosen to give accurate numerical results up to a distance, typically around 40 fm, where the asymptotic behavior is reached and from then on the asymptotic solutions eqs.(14) and eq.(17) are used.

The accurate low-energy continuum spectrum calculations require integration of the radial equations up to distances of the order of ten times the sum of the scattering lengths. For the $n+n+\alpha$ system this is about 180 fm. Too small basis size and too small maximum distance are both disastrous for the numerical reliability.

In Fig. 1 we show the two (strictly decoupled) angular eigenvalue spectra for 1^- and 2^+ . The structure is complicated at small distances where avoided level crossings are seen. The lowest level has in both cases an attractive pocket unable to bind the system, but still responsible for several resonances. At large distance the structure is simpler as the hyperspherical spectrum is approached. In the computation we use the asymptotic behavior, also shown on Fig.1. This improvement of the procedure is absolutely essential when accurate results are required.

The phase shifts for the cases in Fig. 1 are shown in Fig. 2. The rapid

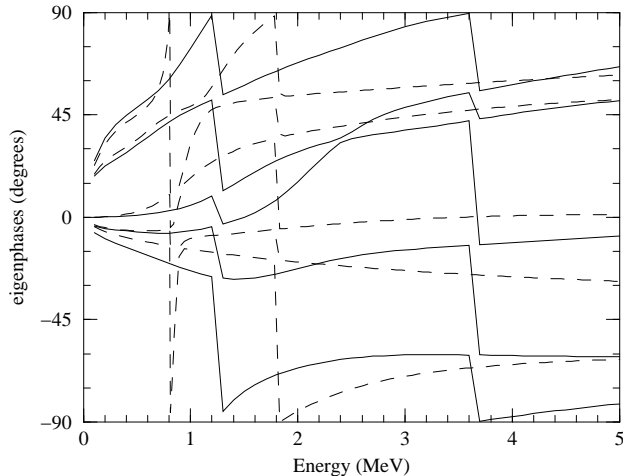


Figure 2: The eigenphases corresponding to the lowest λ -values obtained after diagonalization of the S -matrix for $J^\pi = 1^-$ (solid lines) and $J^\pi = 2^+$ (dashed lines). The interactions are the same as in Fig.1 where a diagonal three-body interaction, $S_3 \exp(-\rho^2/b_3^2)$ with $S_3 = -31$ MeV, $b_3 = 2.061$ fm, is added in all partial waves.

variation and the subsequent crossing of $\pi/2$, seen at four energies, are the traditional signs of resonances. On the other hand it is also possible to have resonance-like structures without phase shifts crossing $\pi/2$. They may still show up as poles of the S -matrix.

In Table 1 we give for a few spins and parities the two lowest S -matrix poles obtained by the complex energy method. The radial equations were integrated numerically up to $\rho_{max}=180$ fm where the $1/\rho^3$ tail of the effective potential becomes negligible. The numerical solutions were then matched at ρ_{max} with the Hankel functions $H^{(\pm)}$. Precisely at the pole only the $H^{(+)}$ function must match the numerical solution. We show the results for two different three-body forces, i.e. fine tuned to the ground state energy and to the 2^+ -resonance. Although the differences appear to be relatively small, they are important for the observable properties. The two cases in Table 1 can be considered to give the realistic range of the possible variation of the three-body force. For angular momentum 0^- , 1^\pm and 2^- the relatively small pocket in the effective radial potential combined with strong centrifugal barrier hinders the effect of the three-body force on the phase shifts and the resonance properties. Apart from the lowest 2^+ state all these resonances reside above the effective centrifugal barrier and must therefore correspond to rather smooth structures in the cross sections.

An observable less sensitive to the large-distance behavior is related to the

Table 1: The real and imaginary values (E_r, Γ) (in MeV) of the two lowest S -matrix poles $E = E_r - i\Gamma/2$ for ${}^6\text{He}$ for various spins and parities. The interactions used are the same as in Fig.1. The three-body interaction parameters are $S_3 = -7.55$ MeV, $b_3 = 2.9$ fm and $S_3 = -31$ MeV, $b_3 = 2.061$ fm respectively for the first two and the last two columns. Correspondingly the excitation energies are $E^* = E_r + 0.95$ MeV and $E^* = E_r + 1.54$ MeV.

J^π	E_r	Γ	E_r	Γ	E_r	Γ	E_r	Γ
0^+	0.94	0.64	1.46	0.83	0.62	0.56	1.16	0.67
0^-	2.07	0.74	-	-	2.07	0.74	-	-
1^+	1.62	0.74	2.55	0.86	1.62	0.74	2.55	0.86
1^-	1.11	0.42	1.67	0.58	0.95	0.38	1.43	0.56
2^+	1.02	0.37	1.23	0.45	0.845	0.093	1.05	0.40
2^-	0.90	0.34	1.82	0.57	0.90	0.34	1.82	0.57

excitations from the ground state. We show in Fig. 3 the lowest three strength functions, $S_{0^+ \rightarrow J^\pi}^\lambda(E)$, as functions of energy both for plane waves and for the proper continuum wave functions. We find 91%, 60% and 70% of the strength below 5 MeV, respectively for monopole, dipole and quadrupole excitations. We notice the usual rise from zero to a maximum and the fall off towards zero at large energy. The peak is very pronounced for 2^+ reflecting the observed resonance of width 0.11 MeV at 0.82 MeV. Above the smooth plane-wave background for 1^- is seen a peak at about 0.95 MeV and a shoulder at about 1.8 MeV. This significant 1^- enhancement is the result of a combination of two overlapping broad resonances, see the S -matrix poles in table 1. It should be detectable although in the same energy region as the 2^+ -resonance. The nuclear 0^+ strength function resembles the plane wave result reflecting broader underlying structures.

Conclusions. We have formulated a method to compute low-energy three-body continuum spectra for arbitrary short-range potentials. It is based on a recent successful method used to calculate bound states by solving the Faddeev equations in coordinate space. The angular part of the equations are treated purely numerically at short distances, whereas the large-distance behavior of eigenvalues and eigenfunctions is computed essentially analytically for all partial waves. Combining the results from these two regions allow accurate computations up to very large distances. Realistic computations for ground state properties, transition matrix elements, phase shifts, resonance energies and widths of $J^\pi = 0^\pm, 1^\pm, 2^\pm$ are carried out for the Borromean halo nucleus ${}^6\text{He}$. The established $J^\pi = 2^+$ resonance is found together with a number of other broader resonances.

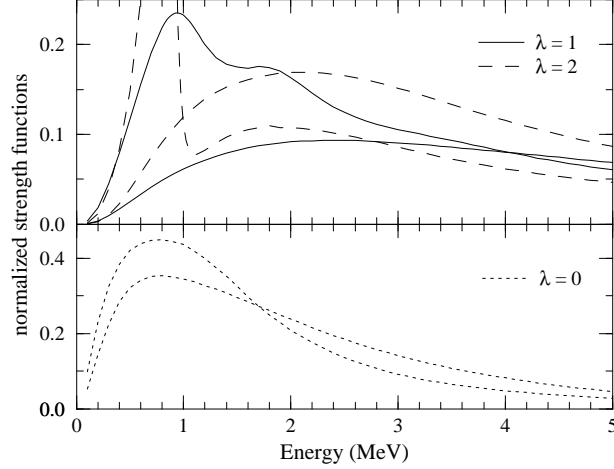


Figure 3: The strength functions, $S^{(\lambda)}(E) = \sum_n |\langle nJ^\pi || M(E\lambda) || 0^+ \rangle|^2$ for ${}^6\text{He}$ as function of energy for transitions from the ground state to 0^+ (dotted), 1^- (solid) and 2^+ (dashed) excited continuum states. The operator is $M(E\lambda, \mu) = \rho^2$ and $\sum_{i=1}^3 q_i r_i^\lambda Y_{\lambda\mu}(\hat{r}_i)$ respectively for $\lambda = 0$ and $1, 2$. The units are the corresponding sum rules $\langle 0^+ | \rho^4 | 0^+ \rangle - \langle 0^+ | \rho^2 | 0^+ \rangle^2 = 749 \text{ fm}^4$ for $\lambda = 0$ and $q_\alpha^2 (2\lambda + 1) \langle 0^+ | r_\alpha^{2\lambda} | 0^+ \rangle / (4\pi) = 1.31e^2 \text{ fm}^2$ and $8.19e^2 \text{ fm}^4$ respectively for $\lambda = 1, 2$, where $q_\alpha = 2e$ is the ${}^4\text{He}$ -charge and r_α is the ${}^4\text{He}$ -distance from the ${}^6\text{He}$ center of mass. The interactions are the same as in Fig.1 with a diagonal three-body interaction added in all partial waves. The parameters are $S_3 = -7.55 \text{ MeV}$, $b_3 = 2.9 \text{ fm}$ for 0^+ and $S_3 = -31 \text{ MeV}$, $b_3 = 2.601 \text{ fm}$ for 1^- and 2^+ . The smooth curves correspond to plane waves for the continuum states.

Acknowledgments. One of us A.C. acknowledges the support from the European Union through the Human Capital and Mobility program contract nr. ERBCHBGCT930320.

References

- [1] W.Glöckle, H.Witala, D.Hüber, H.Kamada and J.Golak, Phys. Rep. **274**, 107 (1996).
- [2] J.L.Friar, Proc. Int. Conf. on Few Body Problems in Physics, Williamsburg 1994, ed. F.Gross, AIP Conference proceedings **334**, 323 (1995).
- [3] J. Carbonell, C. Gignoux, and S. P. Merkuriev, Few-Body Systems **15**, 15 (1993).

- [4] J.L. Friar, G.L. Payne, W.Glöckle, D.Hüber and H.Witala, Phys. Rev. **C51**, 2356 (1995).
- [5] A. Kievsky, S. Rosati, W. Tornow and M.Viviani, Nucl. Phys. **A607**, 402 (1996).
- [6] P.G. Hansen, A.S. Jensen and B. Jonson, Ann. Rev. Nucl. Part. Sci. **45**, 591 (1995).
- [7] D.V. Fedorov, A.S. Jensen, and K. Riisager, Phys. Rev. **C49**, 201 (1994); **C50**, 2372 (1994).
- [8] M.V. Zhukov, B.V. Danilin, D.V. Fedorov, J.M. Bang, I.J. Thompson, and J.S. Vaagen, Phys. Rep. **231**, 151 (1993).
- [9] V.N. Efimov, Comm. Nucl. Part. Phys. **19**, 271 (1990).
- [10] B.D. Esry, C.D. Lin and C.H. Greene, Phys. Rev. **A54**, 394 (1996).
- [11] B.V. Danilin and M.V. Zhukov, Phys. Atom. Nucl. **56**, 460 (1993).
- [12] B.V. Danilin, T. Rogde, S.N. Ershov, H.Heiberg-Andersen, J.S. Vaagen, I.J. Thompson and M.V. Zhukov, Phys. Rev. **C55**, R577 (1997).
- [13] D. V. Fedorov and A. S. Jensen, Phys. Rev. Lett. **71**, 4103 (1993).
- [14] D. V. Fedorov and A. S. Jensen, Phys. Lett. **B389**, 631 (1996).
- [15] D.V. Fedorov, A.S. Jensen and K. Riisager, Phys. Rev. Lett. **73**, 2817 (1994).
- [16] J.R. Taylor, Scattering Theory, (Wiley and Sons, New York 1972) Chapter 20.
- [17] A.S. Jensen, E. Garrido and D.V. Fedorov, Few-Body Systems (in press).
- [18] E. Garrido, D.V. Fedorov and A.S. Jensen, Nucl. Phys. **A 617**, 153 (1997).